

## Defects in Roll-Hexagon Competition

S. Ciliberto,<sup>(1)</sup> P. Coulet,<sup>(2)</sup> J. Lega,<sup>(2),(3)</sup> E. Pampaloni,<sup>(1)</sup> and C. Perez-Garcia<sup>(4)</sup><sup>(1)</sup>*Istituto Nazionale di Ottica, Largo E. Fermi 6, 50125 Firenze, Italy*<sup>(2)</sup>*Laboratoire de Physique Théorique, Université de Nice, Parc Valrose, 06034 Nice CEDEX, France*<sup>(3)</sup>*Department of Mathematics, University of Arizona, Building 89, Tucson, Arizona 85721*<sup>(4)</sup>*Departamento de Física, Facultad de Ciencias, Universidad de Navarra, 31080 Pamplona, Navarra, Spain*  
(Received 7 June 1990)

The defects of a system where hexagons and rolls are both stable solutions are considered. On the basis of topological arguments we show that the unstable phase is present in the core of the defects. This means that a roll is present in the penta-hepta defect of hexagons and that a hexagon is found in the core of a grain boundary connecting rolls with different orientations. These results are verified in an experiment of thermal convection under non-Boussinesq conditions.

PACS numbers: 47.20.Bp, 47.25.Qv

Defects play an important role in the dynamics of pattern-forming systems. Specifically, dislocations and grain boundaries in convective patterns of rolls, and spirals and centered defects in chemical reactions, have been the object of several studies.<sup>1</sup> However, the structure of defects has not been carefully analyzed in systems where two different symmetries coexist. This is a very important case that appears very often in nature, a typical example being the transition between hexagons and rolls in thermal convection. The competition between patterns associated with different symmetries has recently been discussed on the basis of general arguments.<sup>2</sup> The purpose of this Letter is to study defect properties when hexagons and rolls are stable solutions in a nonequilibrium pattern-forming system.

The competition between hexagons and rolls can be described by means of three coupled Ginzburg-Landau equations (GLH), which determine the behavior of the three complex amplitudes  $A_i$  of the sets of rolls describing the hexagonal structure. Each of them makes an angle of  $2\pi/3$  with each of the others. A qualitative description of the nature of the cores of the various defects which may be observed in this problem can be deduced<sup>3</sup> from an elementary study of the following six-dimensional dynamical system, obtained from GLH, in the limit of homogeneous patterns:<sup>4</sup>

$$\partial_t A_1 = \mu A_1 + \alpha \bar{A}_2 \bar{A}_3 - (|A_1|^2 + \gamma |A_2|^2 + \gamma |A_3|^2) A_1, \quad (1a)$$

$$\partial_t A_2 = \mu A_2 + \alpha \bar{A}_3 \bar{A}_1 - (|A_2|^2 + \gamma |A_3|^2 + \gamma |A_1|^2) A_2, \quad (1b)$$

$$\partial_t A_3 = \mu A_3 + \alpha \bar{A}_1 \bar{A}_2 - (|A_3|^2 + \gamma |A_1|^2 + \gamma |A_2|^2) A_3. \quad (1c)$$

The parameter  $\alpha$  describes non-Boussinesq effects. Its sign can be chosen arbitrarily. We assume in the following that  $\alpha$  is positive, and  $\gamma > 1$ , in order to insure the stability of rolls for large values of  $\mu$ . The dynamical

system (1) possesses four kinds of stationary solutions.

(i) The conductive state (O), given by  $\{A_j = 0, j = 1, 2, 3\}$ , is stable for  $\mu < \mu_2 = 0$ , and unstable for  $\mu > \mu_2$ .

(ii) Rolls, given by  $\{A_1 = \sqrt{\mu} \exp[i\varphi_1], A_2 = 0, A_3 = 0\}$  and any circular permutation, are unstable for  $\mu < \mu_3 = \alpha^2/(\gamma - 1)^2$ , and stable for  $\mu > \mu_3$ .

(iii) Hexagons are given by  $\{A_1 = R \exp[i\varphi_1], A_2 = R \exp[i\varphi_2], A_3 = R \exp[i\varphi_3]\}$ , with  $(1 + 2\gamma)R^2 - \alpha R - \mu = 0$  and  $\Phi = \varphi_1 + \varphi_2 + \varphi_3 = 0$  or  $\pi$ . Those associated with  $\Phi = \pi$  exist for positive values of  $\mu$ , and are always unstable. The former exist for  $\mu > \mu_1 = -\alpha^2/4(1 + 2\gamma)$ . The upper branch  $H^+$  (see Fig. 1) is stable only for  $\mu_1 < \mu < \mu_4 = \alpha^2(\gamma + 2)/(\gamma - 1)^2$ ; the lower branch  $H^-$  is always unstable.

(iv) The "mixed states" are given by  $\{A_1 = R \exp[i\varphi_1], A_2 = R \exp[i\varphi_2], A_3 = U \exp[i\varphi_3]\}$  or any circular permutation, with  $U = \alpha/(\gamma - 1)$ ,  $R = [(\mu - U^2)/(1 + \gamma)]^{1/2}$ , and  $\Phi = 0$ . They exist for  $\mu > \mu_3$  and are always unstable.

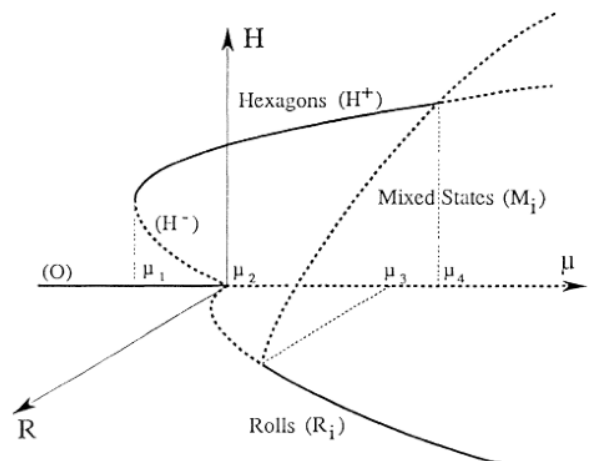


FIG. 1. Stationary solutions of Eqs. (1), in a  $\mu$ -hexagon-roll phase space. The solid lines correspond to stable solutions; dashed lines, to unstable ones. The mixed state  $M_1$  interpolates between rolls and hexagons.

These solutions are given in Fig. 1. They have been observed in several experiments<sup>5,6</sup> and good agreement with theoretical predictions<sup>7</sup> has been found. However, a detailed study of the defects in these patterns is still lacking.

Let us now consider a set of possible initial conditions for Eqs. (1). It can be mapped into a two-dimensional manifold  $\mathcal{M}_i$  in the six-dimensional phase space of the above dynamical system. An initial point of  $\mathcal{M}_i$  lies generically in the basin of attraction of one of the stable stationary solutions, and will evolve towards it under the dynamics. Nevertheless, it may also lie in the stable manifold of one of the unstable stationary solutions. For instance, when many stable solutions are coexisting, some of these manifolds separate the various basins of attraction of the stationary stable solutions. Thus, each time  $\mathcal{M}_i$  intersects a stable manifold of a stationary unstable solution, the dynamics eventually leads to singularities. Indeed, they correspond to loci where the system locally reaches an unstable solution, and are located on points or lines in the physical space  $(x, y)$ . These singularities can be seen as point (dislocations) and line (grain-boundaries) defects, or fronts, and turn out to be real defects or fronts of GLH (namely, when one takes account of spatial inhomogeneities).

In what follows, we apply those considerations to describe the core of the dislocation of a hexagonal pattern, and that of a grain boundary between two sets of rolls which build up this hexagonal pattern. For  $\mu_2 < \mu < \mu_3$ , hexagons  $H^+$  are the only stable stationary solution. Let  $\mathcal{W}_s(S)$  denote the stable manifold of any unstable solution  $S$ , and define  $\mathcal{W}_s = \mathcal{W}_s \cup S$  as its *generalized stable manifold*. If the intersection of  $\mathcal{M}_i$  and  $\mathcal{W}_s$  is not generically empty and is of dimension  $n < 2$ , hexagons will have defects with a core of dimension  $n$ . Moreover, the solution  $S$  will be observed at the core of those defects. For  $\mu_2 < \mu < \mu_3$ , the only stationary unstable solutions whose generalized stable manifold is of dimension greater than 3 are the rolls  $R_j$  (see Fig. 1), with  $j=1, 2, 3$ , and  $\dim[\mathcal{W}_s(R_j)] = 4$ . Thus,  $\mathcal{M}_i$  and  $\mathcal{W}_s(R_j)$  will intersect generically on points. Hence, the defect of a hexagonal pattern is a point defect, at the core of which one observes a roll structure. It is the well-known penta-hepta pair, and can also be pictured as a pair of dislocations on two sets of rolls which build the hexagonal pattern, since two of the amplitudes  $A_i$  vanish.

For  $\mu_4 < \mu$ , rolls  $R_j$  are the only stable solutions. The mixed states  $M_j$  have five-dimensional generalized stable manifolds, which separate the basins of attraction of rolls. The generic intersections between  $\mathcal{M}_i$  and  $\mathcal{W}_s(M_j)$  are lines, which correspond to grain boundaries in the physical space. Thus, the core of a grain boundary between two sets of rolls of a hexagonal structure is characterized by the presence of a mixed state, in which a third roll appears, but with an amplitude weaker than the other two.

When different kinds of stationary solutions are simultaneously stable, the singularities of (1) turn into fronts or defects characterized by a large core. The latter are seeds of nucleation.<sup>8</sup>

A recent experiment on non-Boussinesq convection<sup>6</sup> allows us to verify these considerations in some detail. The system under study is a shallow horizontal layer of pure water heated from below. The layer of depth  $d=0.18$  cm is confined in a cylindrical cell of aspect ratio  $\Gamma=r/d=20$ , where  $r=3.6$  cm is the radius of the cylinder. The bottom heating plate of the cell is made of copper, while the top plate is made of sapphire, allowing for optical inspection. An optical technique, based on the local deflections of a laser beam allows us to measure the vertically averaged temperature field  $T(x, y)$ , produced by the convective motion. More details about the experimental setup may be found in Ref. 6.

The experiment has been performed at the mean working temperature of 28.3°C, where the Prandtl number of water is 5.62 and the horizontal diffusion time is  $\tau_h=2.45$  h.<sup>6</sup> The convective motion appears when the temperature difference  $\Delta T$  between the two horizontal plates is equal to  $\Delta T_c=12.62^\circ\text{C}$ . With such a big  $\Delta T_c$  the temperature dependence of the transport coefficients cannot be neglected (non-Boussinesq conditions) and, therefore, a hexagonal pattern is formed near the convective threshold. When  $\mu=1-\Delta T/\Delta T_c$  is increased, at  $\mu=\mu_4=0.09$  the hexagonal pattern is replaced by a pattern of rolls. Vice versa, the roll-hexagon transition occurs at  $\mu=\mu_3=0.03$  when  $\Delta T$  is decreased.

When a hexagonal pattern is developed, the stationary defects observed in experiments consist of pairs of penta-heptagonal cells.<sup>9</sup> However, in our experiment<sup>6</sup> no penta-hepta pairs were obtained spontaneously. In order to analyze this kind of defect, a penta-hepta pair is induced in some point of the convective pattern by means of some extra heating, obtained by focusing the light coming out of a powerful lamp. Once this defect is induced it remains without variation for a very long time, sufficient to make measurements. In Fig. 2(a) we report the isotherms of  $T(x, y)$  at  $\mu=0.02$ ; only a small portion of the cell is shown in order to amplify the details. The penta-hepta pair is easily observable in the center of the plot [Fig. 2(a)].

Because of the presence of a rather regular hexagonal pattern, the  $T(x, y)$  may be decomposed into the sum of three main sets of rolls:

$$T(x, y) = \sum_{j=1}^3 A_j(x, y) \exp(i\mathbf{K}_j \cdot \mathbf{x}) + \text{c.c.}, \quad (2)$$

where all the information about the defect is contained in the slowly varying amplitudes  $A_j(x, y)$ , and the wave vectors  $\mathbf{K}_j$  have the modulus equal to the critical wave vector  $K_c$ . To obtain the amplitudes  $A_j$  we first compute the Fourier transform  $F(K_x, K_y)$  of  $T(x, y)$ . The Fourier spectrum  $S(K_x, K_y) = |F|^2$  presents six peaks [Fig.

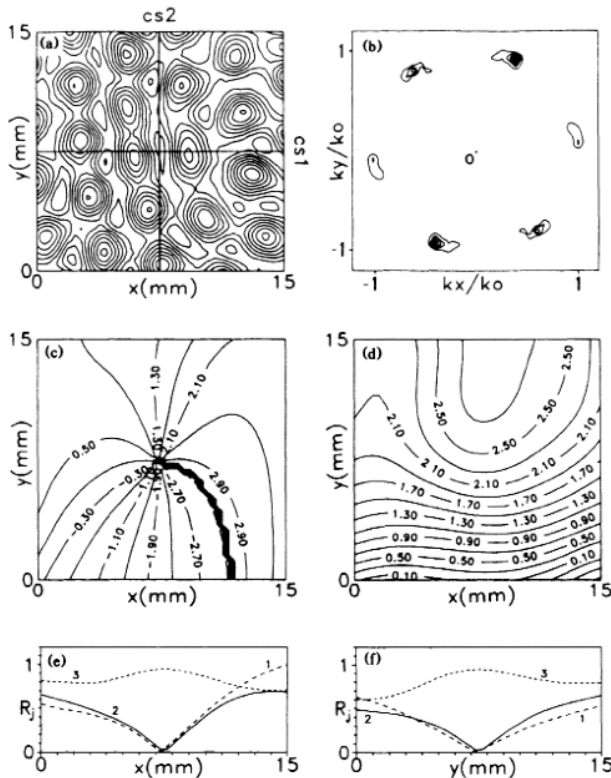


FIG. 2. Defect in a pattern of hexagons: penta-hepta pair. (a) Isotherms of the convective temperature field  $T(x,y)$  in a small area of the cell at  $\mu=0.02$ . (b) Spatial Fourier spectrum of the field in (a). (c) Equiphasal lines of  $\varphi_1$ . (d) Equiphasal lines of  $\varphi_3$ . (e) Cross sections of the amplitudes  $R_j$  with  $j=1-3$  along the line labeled CS1 in (a). (f) As in (e) but the cross sections are done along CS2 in (a).

2(b)], whose centers of mass are at the vertices of the vectors  $\mathbf{K}_j$  and  $-\mathbf{K}_j$ . These vectors are disposed on a hexagon in Fourier space (Fig. 2). Once the  $\mathbf{K}_j$  are determined, we consider first peak 1 and we shift  $F(K_x, K_y)$  by  $-\mathbf{K}_1$ ; thus peak 1 is centered in the origin. We filter out the contributions of all the other peaks by multiplying the shifted  $F(K_x, K_y)$  by a low-pass filtering function (Hamming window)<sup>10</sup> having a suitable cutoff in the range of the peak width. Finally, we anti-Fourier transform to get the complex amplitude  $A_1(x,y)$  of the first set of rolls. We repeat the same procedure (shift of  $-\mathbf{K}_j$ , low-pass filtering and antitransforms) for the two other sets of rolls. An easy calculation allows us to have the real amplitude  $R_j$  as well as the phase  $\varphi_j$  for the three sets of rolls that form the hexagonal pattern.

In Figs. 2(c) and 2(d), the two phases  $\varphi_1, \varphi_3$  are shown. We notice that in the core of the defect, i.e., in the common side of penta-hepta cells,  $\varphi_1$  has a gap of  $+2\pi$  around the core of the defect. The phase  $\varphi_3$  has instead no singularity. The phase  $\varphi_2$  of the third mode has the same behavior as  $\varphi_1$  but has a jump of  $-2\pi$ ; as a

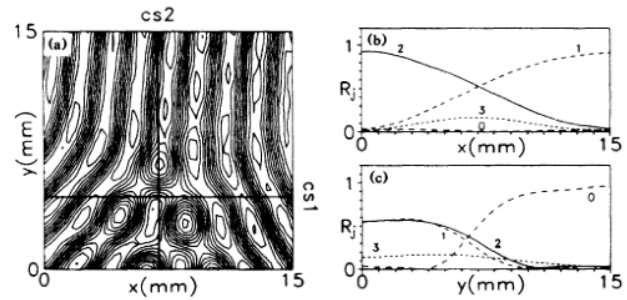


FIG. 3. Defect in a pattern of rolls: grain boundary. (a) Isotherms of the convective temperature field  $T(x,y)$  in a small area of the cell at  $\mu=0.15$ . (b) Cross sections of the amplitudes  $R_j$ , with  $j=0-3$ , along the line labeled CS1 in (a). (c) As in (b) but the cross sections are done along the line labeled CS2 in (a).

consequence it is confirmed that the sum  $\Phi$  of the three phases is zero also in the defect. The jump of  $\pm 2\pi$  in the phases of two sets of rolls indicates that there is a dislocation in each of the two set of rolls 1 and 2. This is confirmed by taking the amplitude  $R_j$  along some lines that cross the singularity [lines labeled CS1 and CS2 in Fig. 2(a)]. The results are shown in Figs. 2(e) and 2(f), where one can see that, far from the defect, the three amplitudes are almost equal; i.e., they form a homogeneous hexagonal pattern. In contrast, in the core of the penta-hepta pair, the two moduli  $R_1$  and  $R_2$  go to zero, whereas the third one,  $R_3$ , increases locally in this region. This means that locally one has a pure roll in the core of the defect; i.e., the unstable solution appears in the defect of the stable solution.

On the other hand, when the pattern of rolls is well developed, some grain boundaries with a local hexagonal structure are observed (this defect is very stable and remains without variation for more than  $140\tau_h$ ). The set of rolls in this experiment is always rather regular in the center of the cell. There are only a few grain boundaries produced by the readjustment of the rolls in the cylindrical container. We analyze now the core of one of these grain boundaries. The isotherms around it are reported in Fig. 3(a); as in Fig. 2(a) only a small portion of the cell is shown.

Here we may divide Fig. 3(a) into an upper and a lower domain. In the former we see that there is a regular set of rolls almost parallel to the  $y$  direction; let us call the slowly varying amplitude of this set of rolls  $A_0$ . Instead, in the lower domain in Fig. 3(a), we have two other sets of rolls, one on the right, whose amplitude is  $A_1$ , and one on the left, with amplitude  $A_2$ . They join themselves to the upper domain and form an angle of about  $\pi/3$  between them. By making the Fourier spectrum of the pattern of Fig. 3(a) we notice the presence of eight peaks, indicating the existence, in the lower domain, of another set of rolls (labeled 3) not observable

in Fig. 3(a). This last set of rolls forms an angle of  $\pi/3$  with sets 1 and 2. The presence of four sets of rolls can be understood by taking into account two systems of GLH, each of them associated with the two above-mentioned domains. We consider the sets of rolls 1 and 2 which form a grain boundary, which is a typical defect of a system where there is a hexagon-roll competition.

To study this defect we use the same procedure as for the penta-hepta pair to obtain the slowly varying amplitudes  $R_j$  and the phases  $\varphi_j$  (with  $j=0-3$ ) of the four modes present in this pattern. In Figs. 3(b) and 3(c) we show the amplitudes of the modes along the lines labeled CS1 and CS2 in Fig. 3(a). From Figs. 3(b) and 3(c) one concludes that the amplitude  $R_0$  of the rolls of the upper domain goes to zero in the defect region; thus it does not give any contribution to the defect formation. The amplitude  $R_1$  ( $R_2$ ) has a maximum where  $R_2$  ( $R_1$ ) has a minimum. In the core of the grain boundary where the two sets, 1 and 2, interpenetrate, the amplitude  $R_3$  reaches its maximum, which is smaller than those of the two oblique ones. Therefore, at the core of this typical defect in the pattern of rolls 1 and 2, the hexagonal unstable solution is encountered. Furthermore, we have checked that the phases do not present any singularity, thus confirming that there are no dislocations in the four sets of rolls.

In conclusion, we have shown from topological arguments, and confirmed in an experiment of thermal convection, that the unstable solution appears in the core of the defects of convective patterns where hexagon and roll symmetries are in competition. The penta-hepta pair can be seen locally as a roll, and a grain boundary between two oblique rolls gives rise locally to hexagons. These defects play an important role in the dynamics of the transition between these two symmetries because they become seeds of nucleation for the other phase,<sup>8</sup> as indeed has been observed in this experiment.<sup>6</sup>

This work has been partially supported by the European Economic Community twinning project No. SC1-0035-C. Two of us (P.C. and J.L.) thank A. C. Newell

for his warm hospitality and for helpful discussions. They also acknowledge research support from the Arizona Center for Mathematical Sciences, University of Arizona, where this work has been completed. Three of us (S.C., C.P.G., and E.P.) acknowledge the financial support of the Italy-Spain Integrated Action (No. 46-1989).

---

<sup>1</sup>*Propagation in Systems Far from Equilibrium*, edited by J. E. Wesfreid, H. R. Brand, P. Manneville, G. Albinet, and N. Boccara, Springer Series in Synergetics Vol. 41 (Springer-Verlag, Berlin, 1988); Y. Kuramoto, in *Chemical Oscillations, Waves and Turbulence*, Springer Series in Synergetics Vol. 19, edited by H. Haken (Springer-Verlag, Berlin, 1984); see also J. Lega, thesis, Université de Nice (unpublished), and references quoted therein.

<sup>2</sup>Y. Pomeau, *Physica* (Amsterdam) **D23**, 3 (1986).

<sup>3</sup>P. Couillet and J. Lega (to be published).

<sup>4</sup>L. A. Segel, *J. Fluid Mech.* **21**, 359 (1965); E. Buzano and M. Golubitsky, *Philos. Trans. Roy. Soc. London A* **308**, 617 (1983).

<sup>5</sup>R. P. Behringer and G. Ahlers, *J. Fluid Mech.* **125**, 219 (1982); M. Dubois, P. Bergé, and J. E. Wesfreid, *J. Phys. (Paris)* **39**, 1253 (1978); C. W. Meyer, G. Ahlers, and D. Cannell, *Phys. Rev. Lett.* **59**, 1577 (1987).

<sup>6</sup>S. Ciliberto, E. Pampaloni, and C. Perez-Garcia, *Phys. Rev. Lett.* **61**, 1198 (1988); E. Pampaloni, C. Perez-Garcia, L. Albavetti, and S. Ciliberto (to be published).

<sup>7</sup>F. H. Busse, *J. Fluid Mech.* **30**, 625 (1967); C. Perez-Garcia, E. Pampaloni, and S. Ciliberto, *Europhys. Lett.* **12**, 51 (1990); P. C. Hohenberg and J. Swift, *Phys. Rev. A* **35**, 3855 (1987).

<sup>8</sup>P. Couillet, L. Gil, and D. Repaux, *Phys. Rev. Lett.* **62**, 2957 (1989).

<sup>9</sup>J. Pantaloni and P. Cerisier, in *Cellular Structures in Instabilities*, edited by J. E. Wesfreid and S. Zaleski, Lecture Notes in Physics Vol. 210 (Springer-Verlag, Berlin, 1983).

<sup>10</sup>A. V. Oppenheim and R. W. Schaffer, *Digital Signal Processing* (Prentice-Hall, Englewood Cliffs, NJ, 1975); L. R. Rabiner and B. Gold, *Theory and Applications of Digital Signal Processing* (Prentice-Hall, Englewood Cliffs, NJ, 1974).